Chapter 3

Solar Light Responsive Photoctalytic Degradation of Tetracycline by Reduced Graphene Oxide-Cadmium Sulfide ($\boldsymbol{RGO - CdS}$) Nanocomposite and its Large Area Thin Film Optoelectronic Device Application.

3.1 Introduction

In recent times, extensive use of pharmaceuticals and personal care products ($PPCPs$) like antibiotics, hormones, anaesthetics, preservatives and anti-inflammatory gels and its notable existence in all marine surroundings such as surface water, intake water, sewage water, ground water etc are of great concern to all scientific people [213, 214]. Among these $PPCPs$, Antibiotics are out of the ordinary concern because of their sustainable and wide spread use in human and veterinary medicine. In huge number of Antibiotics, Tetracycline (TC), the second most attractive antibiotic, have been generally used for the treatment of human being against different infectious diseases and also useful for livestock to put a stop to disease and endorse growth and it is considered as the most commonly used antibiotic in countries like USA, China and India [214]. After the use of antibiotics the residue part has left into the environment. The growth and development of antibiotic-resistant pathogens can be attributed by this residue part and make severe problems for ecology, public health as well as aquatic environment. Now to make environment clean by the removal of TC from the polluted water has become the point of interest to a great number of scientists. In recent time, the elimination of this type of antibiotics could not be possible by wastewater treatment, physical adsorption, biological degradation etc. So we need to develop an efficient and cost effective protocol for eliminating TC in the aqueous medium. Owing to its cost effective, operational simplicity and environmentally sustainable process the procedure of photocatalytic degradation of TC has exposed immense efficiency compare to others [215, 216].

Nowadays, semiconductor catalysts have gained special attention towards the dead set against to environmental pollutant [217, 218]. So far, numbers of semiconductor anti pollutant have been synthesized in laboratory, like TiO_2, ZnS, $CdZnS$, $CdSeS$, $CdSe$, $ZnSe$, SnS, PbS, $CdTe$ etc. are used for the photocatalytic degradation of aquatic pollutant. Among them, cadmium sulfide ($E_g\, of\, CdS = 2.42\, eV$) has received significant attention for its prospective role in photocatalytic water splitting and removal of organic dyes [219]. Upon irradiation of light, excitons are generated in the semiconductor materials. Photo-generated exciton gives free carriers after dissociation at the interface. These photo generated carriers have crucial role on photocatalysis phenomena. But the recombination possibility of the electron and hole reduces the performance of the photocatalysts. To this end the formation of hybrid materials with some matrices like graphene, reduced graphene oxide (RGO) and carbon nanotube (CNT) reduces the recombination probability and ultimately enhance the photocatalytic performance of the semiconductor [219, 220]. Nowadays electronic and optoelectronic properties of 2-dimensional ($2D$) reduced graphene oxide (RGO) in the solar spectrum region have received special attention in the field of nano devices. $2D$ RGO sheets can easily attach metals, metal oxides, polymers and semiconductor material due to its surface unevenness, multiple-functioning of oxygen at the edges and irregular structure of RGO sheets [195]. People have successfully engineered multifunctional newer RGO-based electronic materials by anchoring semiconducting optical materials in the basal plane of RGO [221, 222]. Here in this chapter RGO offers an excellent support towards attaching CdS nanomaterial in its basal plane. In such materials, RGO

plays dual role by offering continuous corridor for easy electron transfer as well as impedes the recombination probability among the photon induced free electron-hole existing in the optical nanomaterials. This attachment of RGO plane effectively enhances the charge generation efficiency by hindering the recombination process. Remarkable efforts have been paid towards the synthesis of $RGO - CdS$ nano composites in order to expand its utility as solar cells, photo diodes, photo transistor materials etc. and in other catagory [217]. The photocatalytic performance of $RGO - CdS$ has been reported by different groups [219]. But TC degradation in aqueous solution by $RGO - CdS$ material has been not yet investigated.

Herein, we report the solar light assisted photodegradation of TC antibiotics degradation by $RGO - CdS$. The $RGO - CdS$ catalysts were synthesized by single step, low cost one pot solvothermal method. As-synthesized materials are characterized both structurally and optically. The confirmation of $RGO - CdS$ synthesis and the attachment of CdS on the RGO were endorsed by XRD, TEM and $UV - vis$ studies. The ground state charge transfer through the interface of the CdS and RGO was confirmed by the steady state PL study. The reduction of GO was further confirmed by Raman spectroscopy. $RGO - CdS$ composite exhibited an excellent photocatalytic performance in the solar light. The electronic transport properties of a thin film photodetector, where $RGO - CdS$ acts as an active material were investigated under solar light irradiation, As-synthesized $RGO - CdS$ composite showed brilliant response under visible light irradiation. Besides, the feasible mechanism for better photo response in the composite has also been anticipated.

3.2 Experimental Section

3.2.1 Materials Used

Graphite powder, potassium persulfate [$K_2S_2O_8$], sodium nitrate [$NaNO_3$], phosphorus pentoxide [P_2O_5], sodium hydroxide [$NaOH$], cadmium acetate dihydrate [$Cd(CH_3COO)_2$] thiourea [NH_2CSNH_2] and sodium nitrate [$NaNO_3$] were purchased from Sigma Aldrich, ethylenediamine [$EN, NH_2CH_2CH_2NH_2$], potassium permanganate [$KMnO_4$], hydrogen peroxide [H_2O_2], hydrochloric acid [HCl] , sulfuric acid [H_2SO_4] were purchased from Merck, India. All the materials were of analytical grade and used as received without further purification.

3.2.2 Materials Preparation:

Graphene oxide (GO) was synthesized through modified Hummers method from pre-oxidized graphite. Initially the pre-oxidized graphite was prepared from natural graphite powder as mention earlier. $RGO - CdS$ nanorod hybrid material was synthesized by simple single step one-pot solvothermal technique. In a typical method cadmium acetate and thiourea of a particular ratio was added in a mixed solvent of ethylene diamine (EN) and DI water ($EN : DIW = 2 : 1$). In this solution GO powder was added under vigorous stirring. Then the solution was transferred into a teflon sealed autoclave and kept it for 8 hours at 175^0C inside a preheated furnace. The consequential precipitate after attaining normal condition was separated by centrifugation at $7000\,rpm$ and washed by DIW and ethanol. Then the $RGO-CdS$ sample

was kept in a preheated oven ($60°C$) for 12 hours. Controlled-CdS nanorod sample was prepared by similar protocol in absence of GO. After that both the sample were collected in powder form for our experiment.

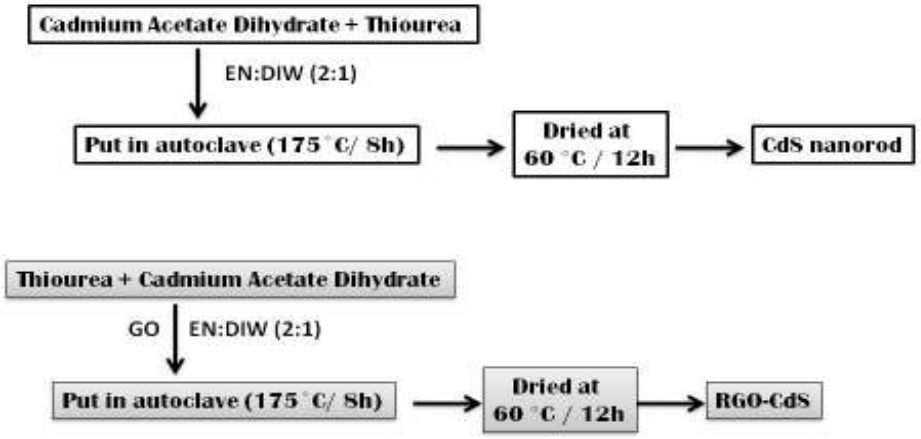

Figure 3.2.1: Synthesis of CdS nano rod and $RGO - CdS$ nano composite

3.3 Charaterisation:

The synthesized materials were characterized structurally and optically by XRD, TEM, $HRTEM$, Raman, $UV - vis$ and PL measurements. The diffraction pattern was collected from a Rigaku Miniflex II X-ray diffractometer with scan rate $10° / min$, with CuK_α radiation ($1.5406\mathring{A}$) respectively. The TEM images were taken by $GEOL$ 2010 operated at $200\,KV$. Raman scattering spectra was recorded on a Jobin-Yvon Horiba ($model$: $T64000$) spectrometer. Shimadzu UV 1700 spectrophotometer was employed

to collect the $UV - vis$ absorption spectra of the synthesized materials. PL spectra were collected from a Perkin Elmer $LS\,55$ spectro fluorometer. The photo catalytic degradation of aqueous TC solution was carried out in a glass photo reactor fitted with solar light simulator (Oriel 67005, Newport) at normal temperature and pressure. To study the optoelectronic transport property, a two terminal photodetector based on $RGO - CdS$ thin film was fabricated by simple drop casting method. The room temperature photocurrent was measured by a Keithly $2612A$ source meter under the irradiation from a solar light simulator (Newport).

3.4 Result and Discussion

Figure 3.4.1A compares the XRD patterns of Graphite, GO, RGO, controlled-CdS nano rod and RGO–CdS nano composite. Here the signature peaks of Graphite and GO are visualised at 26.3° and 10.5° respectively, representing the interlayer spacing of graphite ($0.337\,nm$) increased to $0.882\,nm$ for GO after sufficient oxidation. The peaks observed in the XRD pattern of controlled-CdS are well agreement with our previous reported value and the structure of CdS is hexagonal wurtzite [132]. The sharp peak at $2\theta \approx 26.7^0$ indicates the preferential growth is along (002) direction [217]. All the indexed peaks of the controlled sample are distinctly present in the $RGO-CdS$ composite. No peak shift has been observed, implies that the presence of RGO does not make any significant change in the crystalline phase of CdS [221].

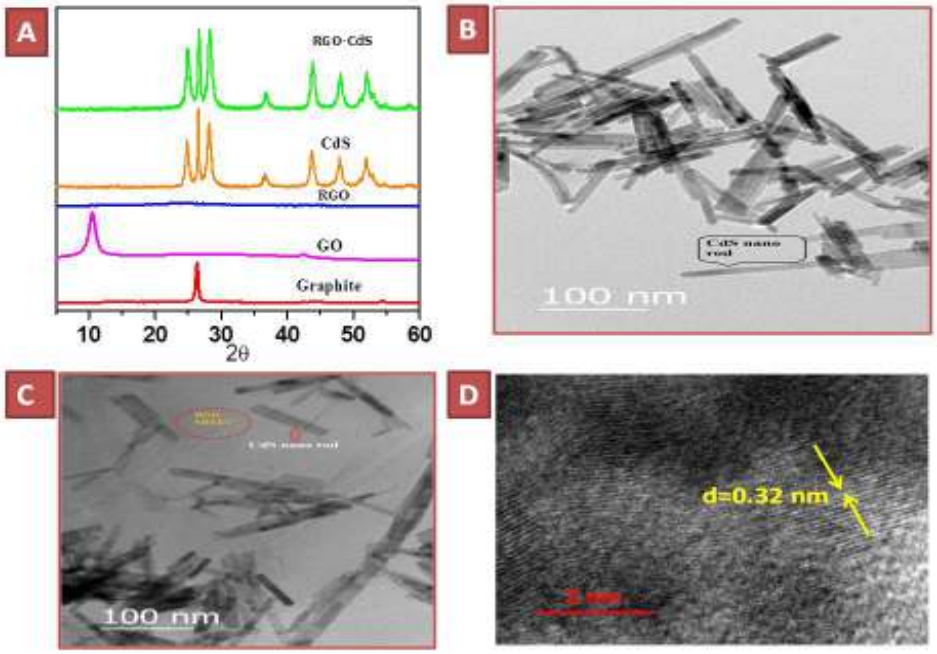

Figure 3.4.1: (A) XRD patterns of Graphite, GO, RGO, CdS, and $RGO - CdS$ composite. TEM images of (B) CdS and (C) $RGO - CdS$ composite (D) HRTEM image of $RGO - CdS$ composite.

The morphological confirmation of CdS was deeply sense by TEM imaging and is presented in Figure 3.4.1B. Nanorod morphology of the CdS with lengths and widths in the range of 150–250 nm and 10–15 nm respectively is observed. From $HRTEM$ (Figure 3.4.1D) we have calculated the lattice fringe spacing as well as inter layer distance of $CdS \approx 0.33\,nm$. $HRTEM$ and XRD studies unambiguously show high crystallinity of CdS-nanorods with crystal planes oriented perpendicular to the nanorod axes. Figure 3.4.1C shows that the controlled-CdS nano rod are well attached with the RGO plane. TEM and $HRTEM$ studies also indicate the preferential growth direction of the nanorod is along (002) direction which is well agreement with the XRD data.

The reduction of GO and formation of $RGO-CdS$ composite were confirmed and Raman spectroscopy (Figure 3.4.2A). The optical properties of controlled-CdS and $RGO-CdS$ nano materials were studied by UV–Vis and PL. A comparison of the $UV-vis$ spectra of both the controlled-CdS nanorod and $RGO-CdS$ composite is compared in Fig. 3.4.2B. A band at around $490\,nm$ in the absorption spectrum of controlled sample is observed. The bandgap energy of the controlled-CdS nanorod as calculated by extrapolating the straight portion of $(\alpha h\upsilon)^2$ versus photon energy $(h\upsilon)$ curve to $\alpha = 0$ (Figure 3.4.2C), using Kubelka–Munk function is $2.42\,eV$. The absorption peak of CdS at $490\,nm$ became weaker and broader in $RGO-CdS$ composite. An enhancement of overall absorption in the visible region ranging from $200\,nm$ to $700\,nm$ is observed in $RGO-CdS$ which makes the composite as a solar light responsive catalyst. The PL emission of CdS and $RGO-CdS$ composite were performed for an excitation wavelength of $375\,nm$ and emission was recorded between 470 to $615\,nm$.(Figure 3.4.2D) The PL intensity for CdS-nanorods remarkably quenched after the embodiment of nanorods on the RGO sheets which represents the occurrence of photo induced charge transfer mechanism at the CdS nanorod and RGO interface.

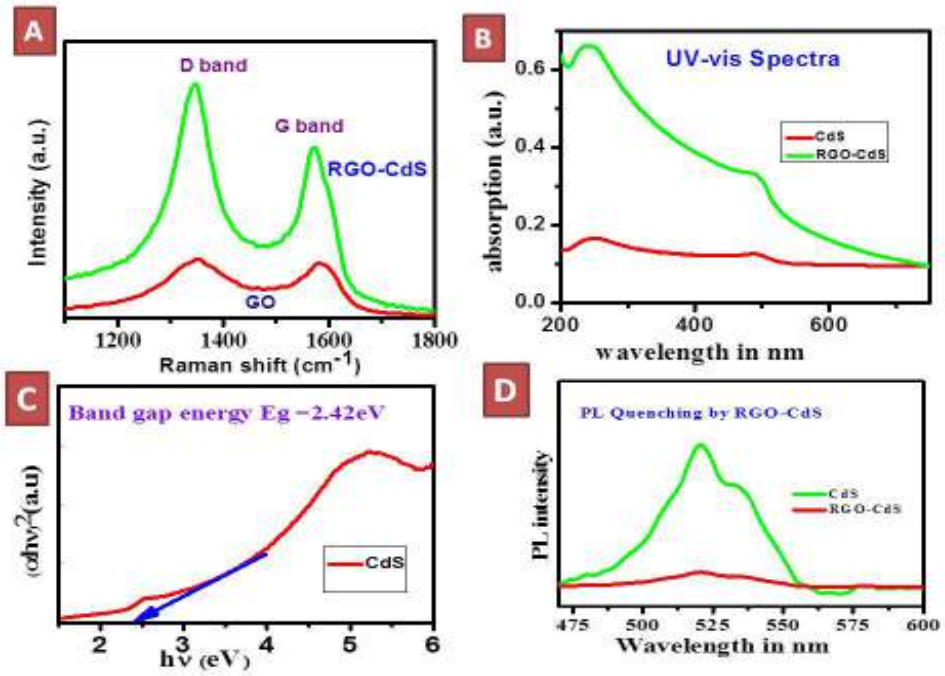

Figure 3.4.2: (A) Raman spectra of GO and $RGO - CdS$. (B) Optical absorption spectra of CdS and $RGO - CdS$. (C) Plot of $(\alpha h\nu)^2$ vs $h\nu$ for CdS. (D) Photoluminescence spectra of controlled-CdS and $RGO - CdS$ nano composite

A significant PL quenching is observed after successful anchoring of CdS nano rod on the top of RGO sheet and that also indicates photo induced charge transformation through the junction of nano rods and RGO sheets during embodiment. $UV - Vis$ and PL study jointly establish the possibility of better photo induced charge generation and better optoelectronic properties of the $RGO - CdS$ composite.

3.5 Applications

3.5.1 Photocatalytic Degradation of Tetracycline:

The room temparature photocatalytic performance of the $RGO-CdS$ nano composite towards the degradation of aqueous Tetracycline (TC) antibiotics solution under visible light was studied extensively. We have also compored with the performance of controlled-CdS nano rod under identical experimental condition.

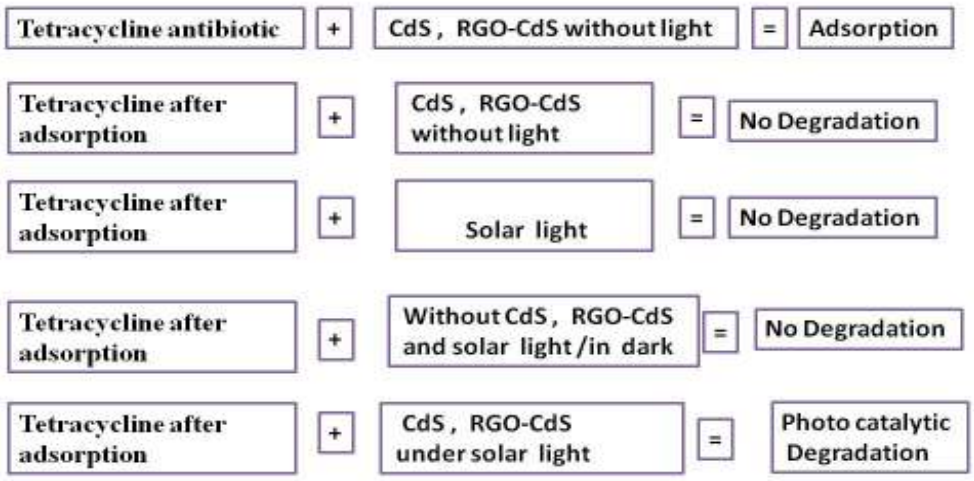

Figure 3.5.1: Steps of photocatalytic procedure

The photocatalytic phenomena was monitored by $UV-Vis$ spectrometered and the density of TC was calculated by the signature peak intensity of TC at $356\,nm$. Initially the TC solution of concentration $0.08\,mmol$ was prepared. The photocatalytic protocol steps one by one are illustrated in figure

3.5.1. In absence of any catalyst and under darkness the absorption peak intensity of the TC solution was noted.Then $40\,mg$ of $RGO-CdS$ catalysts was added in $40\,ml$ TC solution with constant stirring. The catalysts added TC solution was kept under darkness to attain the adsorption-desorption equilibrium. The absorption spectra of TC before and after adsorption-desorption (30 $min.$) in presence of $RGO-CdS$ and controlled-CdS are presented in Figure 3.5.2A and 3.5.2B. So the adsorption efficiency of $RGO-CdS$ and controlled-CdS catalyst are 13 % and 7.34 % respectivly.

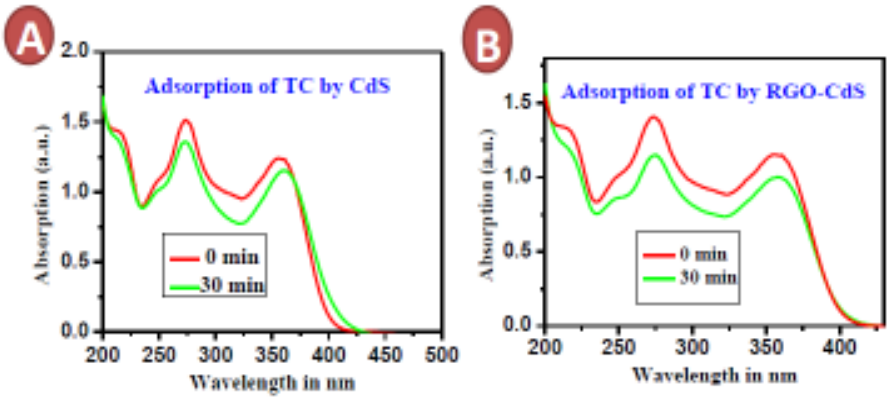

Figure 3.5.2: Adsorption capacity of (A) Controlled-CdS and (B) $RGO-CdS$ nanocomposite

It was observed that the intensity of the TC peak decreased dramatically within $16\,min$ of the irradiation of light. The absorption of TC degradation in presence of CdS and $RGO-CdS$ are presented in figure 3.5.3A and figure 3.5.3B for clearly visualization. The peak intensity after adsorption-desorption equilibrium was considered as the intensity of $0\,min$ (C_0). After shing light the samples were collected and monitor through $UV-vis$ measurement in $2\,min$ intervals. The photocatalytic degradation efficiency

was calculated by the equation 2.4.4 [221]. The degradation efficiency of $RGO - CdS$ and controlled-CdS are compared in figure 3.5.3C. As shown in figure the degradation effficiency of $RGO - CdS$ is 83.25 % within 16 min of irradiation wherw as , it is only 60 % for controlled-CdS under identical experimental condition.

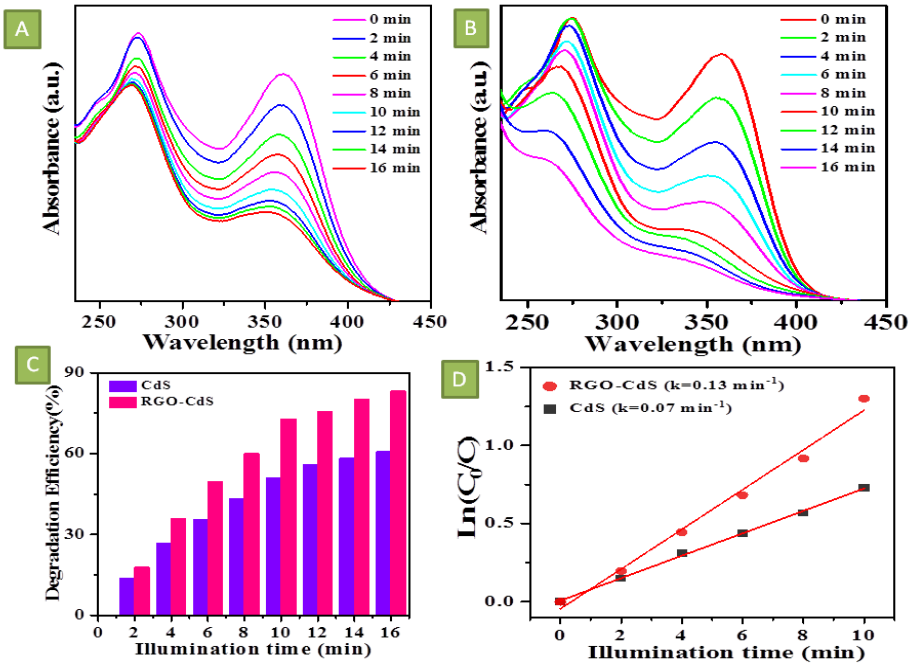

Figure 3.5.3: $UV - vis$ **absorption spectra of aqueous** TC **solution with (A)** CdS **and (B)** $RGO - CdS$ **composite for different illumination time. (C) Comparison of photo degradation efficiency and (D) plot of** $ln(C_0/C)$ **as a function of illumination time for controlled-**CdS **and** $RGO - CdS$ **composite.**

Figure 3.5.3D compares the variation of $ln(C_0/C)$ with radiation time (t) for both $RGO - CdS$ composite and controlled-CdS nanorod. A linear variation indicates the occurrence of pseudo-first-order degradation reaction

in TC by the photocatalyst. The calculated k values are 0.13 and 0.07 min^{-1} for $RGO - CdS$ and CdS respectively towards TC degradation. We have tested that the photocatalytic efficiency of $RGO-CdS$ was unaffected after 5 times re-use **(figure** 3.5.4**)**. The higher photocatalytic degradation efficiency of $RGO - CdS$ composite compare to controlled-CdS nanorod attributed as the efficient separation of electrons and holes through the channel of RGO plane.

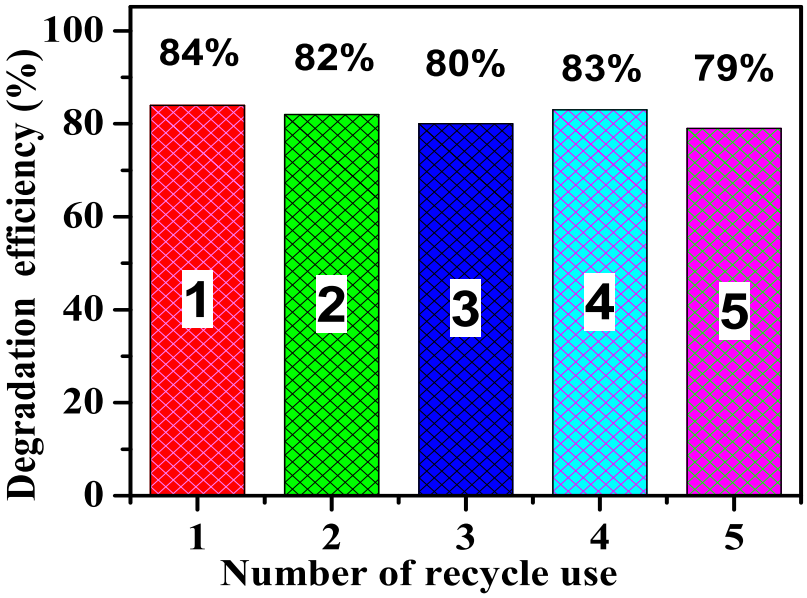

Figure 3.5.4: Recycle use of $RGO - CdS$ as photocatalyst

3.5.2 Opto-Electronic Application:

The device architecture for optoeletronic application is shown in figure 3.5.5A. The two electrodes were drawn by silver paint. Figure 3.5.5C shows the current-voltage characteristics of $RGO - CdS$ nano composite for different

intensity of solar light ($100\,mW/cm^2\,to\,150\,mW/cm^2$) and in darkness. The $I-V$ characteristics of controlled-CdS with the incidence of different intensity of solar light and in dark condition are graphically represented in figure 3.5.5B. A linear variation of current with the applied voltage is observed. The current jumps from $0.64\,\mu A\,to\,1.033\,\mu A$ from dark to solar light irradiation of $150\,mW/cm^2$ intensity at the bias voltage of $2\,volt$ in case of $RGO-CdS$ nano composite thin film. We have also calculated the photosensitivity P (the ratio of photocurrent to dark current), a figure of merit of the photodetector.

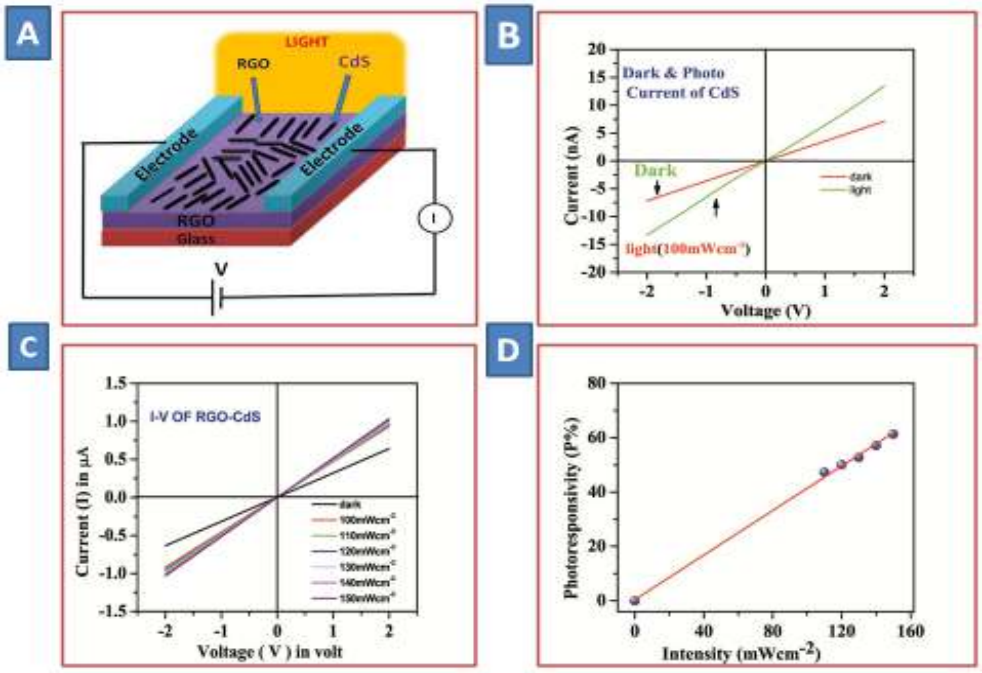

Figure 3.5.5: (A)The cartoon of our photodetector device along with the electrical transport measurement setup. (B) $I-V$ characteristics for controlled-CdS thin film device under dark and different illumination intensity. (C) $I-V$ characteristics for $RGO-CdS$ nanocomposite thin film device under dark and different illumination intensity. (D) The variation of photo sensitivity with illumination intensity of our thin film device.

P of our device varies linearly with the intensity of the light (Figure 3.5.5D) which is also advantageous for making different optoelectronic device application. The linear variation can be explained by the equation 2.4.1. We have calculate that the P in increased upto 61 % at the light intensity of $150\,mWcm^{-2}$. The photocurrent generation in $RGO-CdS$ composite can be explained with the help of the excitonic picture. Under illuminated condition excitons, a pair form of electron and hole, are formed in CdS nano rod that afterwards separates in free electron and hole carriers at the interface of $RGO\ and\ CdS$. In CdS nanorod although electron and hole are formed but they have the tendency to recombine easily and hence it is less photoresponsive. In case of $RGO-CdS$ nano composite material due to favourable band matching of CdS and RGO the photogenerated electrons diffuse to the positive electrode by the interconnected RGO channels while the holes transfer from the valence band (VB) of CdS to the negative electrode. In this way the recombination process has been interrupted and gives high photoresponse property of $RGO-CdS$ composite.

3.6 Conclusion

In conclusion, the novel photo catalyst $RGO-CdS$ nano composite was efficiently synthesized by one pot solvothermal technique. The structure and morphology of as synthesised materials was examined by XRD and TEM measurement. The PL study confirms the photo induced charge transfer through the interface of CdS and RGO. The reduction of GO was further confirmed by Raman spectroscopy. $RGO-CdS$ composite exhibited an ex-

cellent photocatalytic performance in the solar light towards the degradation of TC. The degradation rate constant of $RGO - CdS$ is $0.13\,min^{-1}$, which is nearly 2 times higher compared to controlled-CdS. The significant PL of CdS nanorods after the lapping of RGO sheet confirms the occurrence of better photo-induced charge generation along the junction of RGO and CdS. Thus RGO plays a crucial role for efficient charge separation by hindering the electron-hole recombination probability and finally enhanced the photocurrent in the composite material in solar light irradiation. In the composite, RGO plays a decisive role towards efficient photo induced charge separation and improves the photocatalytic activity of the $RGO - CdS$ composite.